Structural Engineering and Mechanics, Vol. 35, No. 2 (2010) 175-190
DOI: http://dx.doi.org/10.12989/sem.2010.35.2.175

New decoupled wavelet bases for multiresolution structural analysis

Youming Wang, Xuefeng Chen*, Yumin He and Zhengjia He

State Key Lab for Manufacturing Systems Engineering, Xi'an Jiaotong University, Xi'an 710049, People's Republic of China

(Received July 1, 2008, Accepted January 6, 2010)

Abstract. One of the intractable problems in multiresolution structural analysis is the decoupling computation between scales, which can be realized by the operator-orthogonal wavelets based on the lifting scheme. The multiresolution finite element space is described and the formulation of multiresolution finite element models for structural problems is discussed. Various operator-orthogonal wavelets are constructed by the lifting scheme according to the operators of multiresolution finite element models. A dynamic multiresolution algorithm using operator-orthogonal wavelets is proposed to solve structural problems. Numerical examples demonstrate that the lifting scheme is a flexible and efficient tool to construct operator-orthogonal wavelets for multiresolution structural analysis with high convergence rate.

Keywords: multiresolution finite element; lifting scheme; operator-orthogonal wavelet.

1. Introduction

In the last several years, finite element method (FEM) has been recognized as a widely popular method for numerical analysis of differential equations, engineering problems, etc. However, traditional FEM has many disadvantages, i.e., re-meshing initial elements, low efficiency, ill-conditioned matrix, etc. The wavelet-based algorithm is a very good method to solve multiscale problems for its advantages, i.e., multiresolution analysis, orthogonalization, vanishing moments, etc. The combined method called wavelet finite element method has been studied by many researchers because wavelet finite element method has many advantages in numerical computation (Ma *et al.* 2003, Chen *et al.* 2004, Xiang *et al.* 2007).

Traditional wavelets are constructed by scaled and shifted versions of a single mother wavelet on a regularly spaced grid over a theoretically infinite or periodic domain. The main disadvantage of these wavelets is that they can not be constructed on finite domains, i.e., finite meshes commonly encountered in FEM analysis. Therefore, it is very desirable to build new kinds of wavelets that can be defined in general domains or on irregular meshes. Second-generation wavelets based on the lifting scheme (Sweldens 1997) were developed to eliminate the restriction and deficiency of traditional wavelets appropriately. The second generation wavelets form Riesz bases for L_2 space,

*Corresponding author, Ph.D., E-mail: xautroland@163.com

which are local in both space and frequency and have many vanishing polynomial moments without the translation and dilation invariance of their biorthogonal cousins. The numerical performance of second generation wavelet has gained much attention by many researchers. Pinho *et al.* (2004) discussed a multiresolution analysis for the discretisation of Maxwell equations via second generation wavelets. Vasilyev and Kevlahan (2000) established adaptive multilevel collocation method to solve partial differential equations (PDE) over complex geometries using lifted interpolating wavelets. Davis and Strela (1999) proved that all biorthogonal multiwavelet bases can be attained by applying a finite sequence of simple lifting steps to a simple initial basis and generalized lifting scheme to the construction of multiwavelets. Castrillón-Candás and Amaratunga (2003) developed spatially multiwavelets using the lifting scheme to represent integral operators sparsely on general geometries. Sudarshan and Amaratunga (2006) presented approximate Gram-Schmidt orthogonalization method to construct operator-orthogonal wavelets efficiently. Recently, He *et al.* (2007) described a construction method of scale-decoupled wavelets by designing suitable prediction coefficients and update coefficients based on the lifting scheme.

All the construction methods discussed above are focused on the differential equations; however, the numerical performance of structural problems has not investigated. The goal in this paper is to construct various lifted wavelet bases for the structural analysis and verify their numerical performance.

An outline of the paper is as follows. Section 2 introduces multiresolution finite element space based on the property of wavelet multiresolution analysis. Section 3 investigates the construction of multiresolution finite element models for two typical structural problems. Section 4 describes the lifting scheme to construct operator-orthogonal wavelets and the decoupling condition of multiresolution algorithm. A dynamic multiresolution algorithm using lifting wavelets is also presented to solve structural problems. Section 5 demonstrates the numerical performance of the proposed method and conclusions are drawn in Section 6.

2. The multiresolution finite element space

2.1 Multiresolution analysis

Multiresolution analysis (MRA) is the basic important aspect of wavelet-based numerical algorithm, which enables us to handle effectively rapid local-solution variations. A multiresolution analysis is composed of a set of closed subspaces $V_j \in L^2(R)$ with $j \in Z$ and satisfies the following properties (Sweldens 1997):

(1) $V_j \subset V_{j+1}$,

(2) $\cup_{j \in J} V_j$ is dense in L_2,

(3) for each $j \in J$, V_j has a Riesz basis given by scaling functions $\{\phi_{j,k} | k \in K(j)\}$,

where j is the level of resolution, $J \in Z$ is an integer index set associated with resolution levels, $K(j)$ is some index set associated with scaling functions of level j, V_j denotes approximation spaces of level j. For each V_j, there exists a complement of V_j in V_{j+1}, namely as W_j. Let the spaces W_j be spanned by wavelets, $\varphi_{j,m}(x)$ for every $m \in M(j)$, $M(j) = K(j+1)/K(j)$, where $M(j)$ is the difference set of $K(j+1)$ and $K(j)$.

2.2 Multiresolution finite element space

In the multiresolution finite element space, scaling functions are identical to the interpolating functions used in the finite element method. The wavelet functions are chosen to be detail functions in the complementary space of the interpolating functions. A multiresolution decomposition of a finite element space V_j at different levels of resolution is spatial hierarchy:

$$V_j = W_{j-1} \oplus V_{j-1} = W_{j-1} \oplus W_{j-2} \oplus \ldots \oplus W_0 \oplus V_0$$

The definition of multiresolution analysis implies that for every scaling function $\phi_{j,k}$ and wavelet $\varphi_{j,m}$, there exist a group of filter coefficients $\{h_{j,k,l}, j \in J, k \in K(j), l \in K(j+1)\}$ and another filter coefficients $\{r_{j,m,l}, j \in J, m \in M(j), l \in K(j+1)\}$ such that

$$\phi_{j,k} = \sum_l h_{j,k,l} \phi_{j+1,l} \tag{1}$$

$$\varphi_{j,m} = \sum_l r_{j,m,l} \phi_{j+1,l} \tag{2}$$

Eq. (1) and Eq. (2) is referred to as the refinement equations for second generation wavelets. Consequently, the refinement equation between the scaling functions at different levels is

$$\phi_{j,k} = \phi_{j+1,k} + \sum_m h_{j,k,m} \phi_{j+1,m} \tag{3}$$

where $\phi_{j+1,m} = \varphi_{j,m}$ holds in the multiresolution analysis (Sweldens 1997). Eq. (3) implies that for a given function $f_{j+1} \in V_{j+1}$, it can be decomposed by MRA into its projection on a coarse approximation space V_0 along with the projections at multiple levels of wavelet spaces, the refinement relation can be given as

$$f_{j+1} = \sum_{l \in K(j+1)} c^T_{j+1,l} \phi_{j+1,l} = \sum_{k \in K(0)} c^T_{0,k} \phi_{0,k} + \sum_{i=0}^{j} \sum_{m \in M(j)} d^T_{i,m} \varphi_{i,m} \tag{4}$$

where $c_{0,k}$ and $d_{i,m}$ are the projection coefficients of $f(x)$ in the space V_0 and W_j respectively. Eq. (4) is the theoretical foundation of multiscale computation.

In the following, we describe the refinement equations of the scaling functions in the multiresolution finite element space, which are derived by a set of equations consisting of several sample point values of scaling functions and wavelets in the similar form as Eq. (3)

$$\Phi_{j+1,k} + \sum_m h_{j,k,m} \Phi_{j+1,m} = \Phi_{j,k} \tag{5}$$

where $\Phi_{j+1,k}$ and $\Phi_{j+1,m}$ are the sample point values of scaling functions and wavelets at level $j+1$. The refinement relation of a linear interpolating function in Lagrange multiresolution finite element space can be derived by Eq. (5) in the form

$$\phi_{j,k_2} = \phi_{j+1,k_2} + \frac{1}{2}(\phi_{j+1,m_1} + \phi_{j+1,m_2}) \tag{6}$$

which is shown in Fig. 1. If we extend the multiresolution analysis to generalized multiresolution finite element space with higher-order interpolating functions, we can derive many new higher-order wavelets. As a typical example, the refinement equations for quadratic interpolating functions

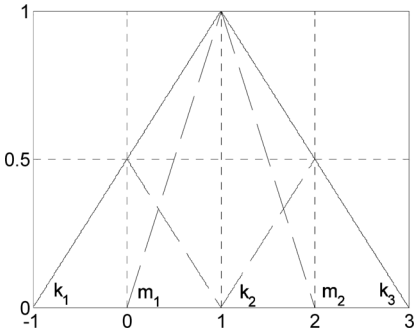

Fig. 1 The refinement relation for a linear interpolation function

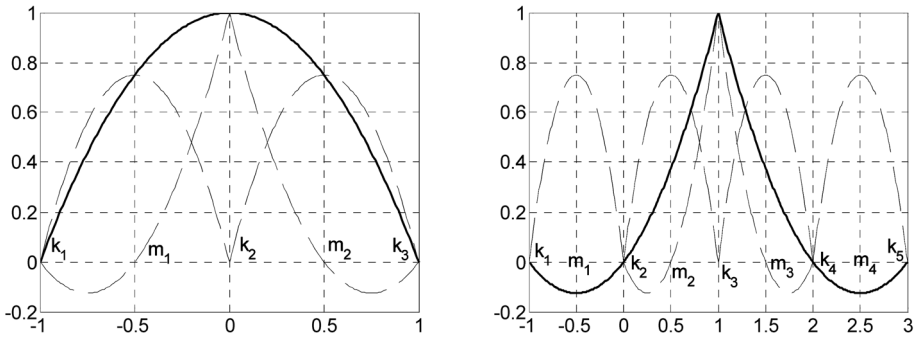

Fig. 2 The refinement relation for quadratic interpolating functions

(Castrillón-Candás and Amaratunga 2003) are

$$\phi_{j,k_2} = \phi_{j+1,k_2} + \frac{3}{4}(\phi_{j+1,m_1} + \phi_{j+1,m_2}) \tag{7}$$

$$\phi_{j,k_3} = \phi_{j+1,k_3} - \frac{1}{8}(\phi_{j+1,m_1} + \phi_{j+1,m_4}) + \frac{3}{4}(\phi_{j+1,m_2} + \phi_{j+1,m_3}) \tag{8}$$

Fig. 2 illustrates the refinement relation for the quadratic interpolation function, the left figure illustrates the piecewise interpolating functions at the end point of two elements and the right figure shows the interpolating functions at the center of a element. On the analogy of Eq. (5), we can derive the refinement relation for cubic interpolation functions in the form

$$\phi_{j,k_2} = \phi_{j+1,k_2} + \frac{15}{16}\phi_{j+1,m_1} + \frac{9}{16}\phi_{j+1,m_2} - \frac{5}{16}\phi_{j+1,m_3} \tag{9}$$

$$\phi_{j,k_3} = \phi_{j+1,k_3} - \frac{5}{16}\phi_{j+1,m_1} + \frac{9}{16}\phi_{j+1,m_2} + \frac{15}{16}\phi_{j+1,m_3} \tag{10}$$

$$\phi_{j,k_4} = \phi_{j+1,k_4} + \frac{5}{16}(\phi_{j+1,m_1} + \phi_{j+1,m_6}) - \frac{1}{16}(\phi_{j+1,m_2} + \phi_{j+1,m_5}) + \frac{1}{16}(\phi_{j+1,m_3} + \phi_{j+1,m_4}) \tag{11}$$

Figs. 3(a)-(c) illustrates the refinement relation for the two interpolation functions, which locate at the center and the end of elements.

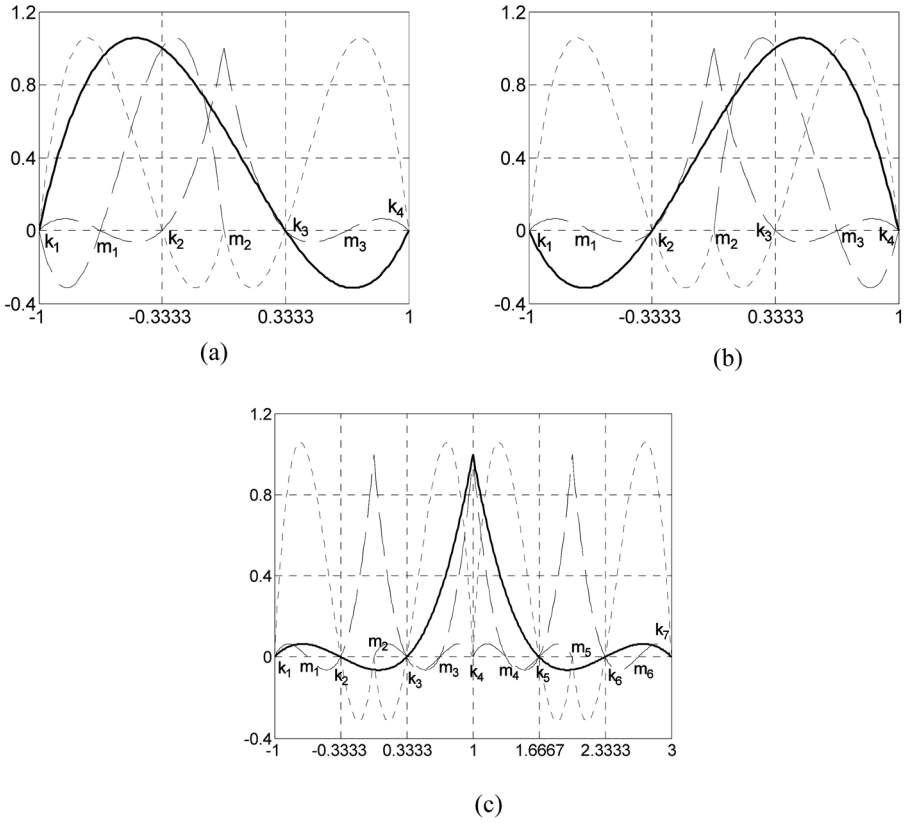

Fig. 3 The refinement relation for cubic interpolating functions

3. The formulation of multiresolution finite element models

In this section we derive the operators of mulresolution finite element models from two typical structural problems including rod and Timoshenko beam problems. More general operators of mutiresolution finite element models, such as two- or three-dimensional finite element models, can be derived similarly and new kinds of operator-orthogonal wavelets can be constructed accordingly.

3.1 Multiresolution rod finite element model

The total potential energy for the finite element models of rods or bars can be expressed as (Wang 2002)

$$\Pi^e = \int_a^b \frac{EA}{2}\left(\frac{du}{dx}\right)^2 dx - \int_a^b f(x)u dx - \sum_i P_i u(x_i) \tag{12}$$

where EA is compressive stiffness, $u(x)$ is axial displacement function, $f(x)$ is distributed loading, element length is $l_e = b - a$, P_i is lump load and x_i is acting position. The finite element approximation of u can be interpolated as

$$u = \phi^e u^e \tag{13}$$

where

$$\phi^e = \{\phi_1^e \ \ \phi_2^e \ \ \dots \ \ \phi_n^e\}$$
$$u^e = \{u_1^e \ \ u_2^e \ \ \dots \ \ u_n^e\}^T$$

Applying the principle of minimum of total potential energy, $\delta\Pi^e = 0$, we can obtain the finite element equation for axial deformation

$$K^e u^e = f^e + P^e \tag{14}$$

Consider finite element models of bars in Lagrange multiresolution finite element space in Eq. (12), the stiffness matrix and the distributed and lump on the multiscale space takes the form

$$K_j^e = \begin{bmatrix} K_j^{e,1} & K_j^{e,2} \\ K_j^{e,3} & K_j^{e,4} \end{bmatrix} = \begin{bmatrix} \int_a^b EA \frac{d\phi_{j,k_1}^T}{dx}\frac{d\phi_{j,k_2}}{dx}dx & \int_a^b EA \frac{d\phi_{j,k_1}^T}{dx}\frac{d\varphi_{j,m_2}}{dx}dx \\ \int_a^b EA \frac{d\varphi_{j,m_1}^T}{dx}\frac{d\phi_{j,k_2}}{dx}dx & \int_a^b EA \frac{d\varphi_{j,m_1}^T}{dx}\frac{d\varphi_{j,m_2}}{dx}dx \end{bmatrix} \tag{15}$$

where k_1, k_2 are nodal number of scaling functions, m_1, m_2 are nodal number of wavelet functions, $K_j^{e,1}$ is the nodal finite element matrix at level j formed by the scaling functions, $K_j^{e,2} = (K_j^{e,3})^T$ is the interaction matrix between the scaling functions and wavelets at level j, $K_j^{e,4}$ is the detail matrix formed by the wavelets at level j. It is noted that given the condition $K_j^{e,2} = (K_j^{e,3})^T = 0$, the multiresolution stiffness matrix will be block-diagonal and sparse, which means that the decoupling multiresolution wavelet computation of structural problems. The elemental distribute loading column vector is

$$f^e = \int_a^b [\phi_{j,k} \ \ \varphi_{j,m}]^T f(x)dx \tag{16}$$

and the lump loading column vector is

$$P^e = \sum_i P_i [\phi_{j,k} \ \ \varphi_{j,m}]^T \tag{17}$$

From Eq. (15), we can define the operator for the finite element models of rods or bars at level j as

$$a(\varphi_{j,m}, \phi_{j,k}) = \int_{-1}^{1} EA \frac{d\varphi_{j,m}^T}{d\xi}\left(\frac{d\phi_{j,k}}{d\xi}\right)d\xi, \quad 0 \le j \le J-1 \tag{18}$$

Considering uniform tension problems of a bar, there is a similar operator by substituting the constant EA. If the operator-orthogonality of rod and bar problems is satisfied, i.e., the operators are zero-valued, the multilevel stiffness matrix will be highly sparse with respect to the principal diagonal. Therefore, the decoupled characteristics of operator-orthogonal wavelets can reduce the computation cost effectively.

3.2 Multiresolution Timoshenko beam finite element model

Consider the influence of shear deformation, the total potential energy functional of Timoshenko beam element $\Omega^e = (x_a, x_b)$ is given

$$\Pi^e = \int_a^b \frac{EI}{2}\left(-\frac{d\theta}{dx}\right)^2 dx + \int_a^b \frac{GAk_s}{2}\left(\frac{dw}{dx} - \theta\right)^2 dx - \int_a^b q(x)w\,dx - \sum_i P_i w(x_i) + \sum_l M_l \theta(x_l) \tag{19}$$

where EI is bending rigidity, G shear modulus, A cross-sectional area, k_s the shear deformation coefficient, $q(x)$ the distributed force, P_i lump forces, M_l lump bending moment, w and θ are the transverse deflection and rotation respectively, x_i and x_l are acting position. The transverse deflection and rotation $w(x)$ and $\theta(x)$ can be interpolated by two Lagrange basis functions, $\phi^{e,1}$ and $\phi^{e,2}$, in the form

$$w(x) = \phi^{e,1} w^e, \quad \theta(x) = \phi^{e,2}\theta^e \tag{20}$$

According to the principle of minimum of total potential energy, $\delta\Pi^e = 0$, we can obtain element solving equations in the multiresolution finite element space in the following

$$\begin{bmatrix} {}^1K^e & {}^2K^e \\ {}^3K^e & {}^4K^e \end{bmatrix} \begin{bmatrix} w^e \\ \theta^e \end{bmatrix} = \begin{bmatrix} P_w^e \\ 0 \end{bmatrix} + \begin{bmatrix} P_{w_i}^e \\ P_{\vartheta_l}^e \end{bmatrix} \tag{21}$$

where ${}^1K^e$-${}^4K^e$ can be denoted by two Lagrange scaling functions and have the similar form as Eq. (15) respectively, the elemental distributed loading column vector is

$$P_w^e = \int_a^b q(x)[\phi^e \quad \varphi^e]^T dx \tag{22}$$

the lump loading column vector

$$P_{w_i}^e = \sum_i P_i[\phi(x_i) \quad \varphi(x_i)]^T \tag{23}$$

and the lump bending column vector

$$P_{\theta_l}^e = -\sum_i M_i[\phi(x_i) \quad \varphi(x_i)]^T \tag{24}$$

The operators of multiresolution Timoshenko beam models can be derived as

$$a_1(\varphi_{j,m}^1, \phi_{j,k}^1) = \int_a^b GAK_s\left(\frac{d\varphi_{j,m}^1}{dx}\right)^T \frac{d\phi_{j,k}^1}{dx} dx \tag{25}$$

$$a_2(\varphi_{j,m}^1, \phi_{j,k}^2) = \int_a^b GAK_s\left(\frac{d\varphi_{j,m}^1}{dx}\right)^T \phi_{j,k}^2 dx \tag{26}$$

$$a_3(\varphi_{j,m}^2, \phi_{j,k}^1) = \int_a^b GAK_s\left(\frac{d\varphi_{j,m}^2}{dx}\right)^T \phi_{j,k}^1 dx \tag{27}$$

$$a_4(\varphi_{j,m}^2, \phi_{j,k}^2) = \int_a^b \left[EI\left(\frac{d\varphi_{j,m}^2}{dx}\right)^T \frac{d\phi_{j,k}^2}{dx} + GAK_s(\varphi_{j,m}^2)^T \phi_{j,k}^2 \right] dx \tag{28}$$

To ensure the operators zero-valued, we will construct two operator-orthogonal wavelets based on the lifting scheme.

4. Dynamic multiresolution algorithm

4.1 The lifting scheme

The lifting scheme presented by Sweldens (1997) constructs a new compact wavelet $\varphi_{j,m}$ by adding the neighboring scaling function to a primitive wavelet $\varphi_{j,m}^{old}$, which is chosen to be a simple scaling function $\phi_{j+1,m}$ from a finer level

$$\varphi_{j,m} = \varphi_{j,m}^{old} - \sum_k s_{j,k,m}\phi_{j,k} = \phi_{j+1,m} - \sum_k s_{j,k,m}\phi_{j,k}, \quad \forall j \text{ and } \forall m \tag{29}$$

where $s_{j,k,m}$ is the lifting coefficients. The lifting scheme gives us more degrees of freedom to custom design operator-orthogonal wavelets by selecting appropriate lifting coefficients $s_{j,k,m}$. According to the operator-orthogonal condition in various structural problems, the lifting coefficients $s_{j,k,m}$ can be determined by computing a basis for the null space of the local interaction matrix Q_j in the form

$$Q_j \begin{bmatrix} -s_{j,k,m} \\ 1 \end{bmatrix} = [a(\phi_{j,k^*}, \phi_{j,k}) \;\; a(\phi_{j,k^*}, \phi_{j+1,k})] \begin{bmatrix} -s_{j,k,m} \\ 1 \end{bmatrix} = 0 \tag{30}$$

where ϕ_{j,k^*} are all the scaling functions on a given domain Ω_j, $\phi_{j,k}$ are the subset of scaling functions that are all interior in the domain Ω_j. It can be inferred that the number of the solution of Eq. (30) determines the number of lifted wavelets. The principle of constructing lifted wavelets is to choose proper lifted coefficients from Eq. (30) such that the lifted wavelets are compactly support and the lifting coefficient vectors are linearly independent.

4.2 Decoupling condition

The vanishing moment of the wavelets is a very important property to ensure the operator-orthgonality between the scaling functions and wavelets, which is also the condition of decouping computation across the scales in the multiresolution finite element space. The vanishing moment concept is defined as follows: if a wavelets φ is piecewise polynomial and satisfies (Mallat 1998)

$$\int_\Omega x^\alpha \varphi dx = 0, \quad \alpha = 0, 1, \ldots, n-1 \tag{31}$$

the wavelet have order-n vanishing moments. Based on the concept of vanishing moments, the operator-orthogonality between the scaling functions and wavelets is discussed as follows. If a

wavelet is continuous piecewise polynomial and is zero-valued at the integration boundary of its support, the derivative of the wavelet will have one vanishing moment. In addition, each vanishing moment in the wavelet will result in an additional vanishing moment in the derivative of the wavelet. The derivation equations are illustrated as

$$\int_{\Omega}\frac{\partial\varphi}{\partial x}dx = \varphi\Big|_{x_1}^{x_2} = 0 \tag{32}$$

$$\int_{\Omega}x\frac{\partial\varphi}{\partial x}dx = x\varphi\Big|_{x_1}^{x_2} - \int_{\Omega}\varphi dx = 0 \Leftrightarrow \int_{\Omega}\varphi dx = 0 \tag{33}$$

$$\int_{\Omega}x^n\frac{\partial\varphi}{\partial x}dx = x^n\varphi\Big|_{x_1}^{x_2} - \int_{\Omega}nx^{n-1}\varphi dx = 0 \Leftrightarrow \int_{\Omega}x^{n-1}\varphi dx = 0 \tag{34}$$

This property is referred to as the inheritance of vanishing moment property (D'Heedene and Amaratunga 2005).

4.3 Dynamic multiresolution algorithm

Firstly, we describe the error estimation for operator-orthogonal wavelet solution. Let e be the error estimate of operator-orthogonal wavelet solution, i.e., the operator-orthogonal wavelet solution u_{j+1} at level $j+1$ with respect to solution u_j at level j in $L^2(R)$ space, then the error estimator e is given (Chen 1995)

$$e = \max|u_{j+1} - u_j| \tag{35}$$

Since the exact solution can not always be found, we adopt a practical and effective error estimate method. Consider u_{j+1} and u_j in the neighbor approximate space, $j+1$ and j, the relative error estimator is

$$\varepsilon_j = \frac{\max|u_{j+1} - u_j|}{\max|u_{j+1}|} \tag{36}$$

The relative error estimator also can indicate the convergence rate of the algorithms. As the scale become larger, it can be ensured that the error estimator satisfies any threshold value.

In the following, we proposed a dynamic multiresolution algorithm using lifted wavelets to the solution of engineering problems:

1) Given a threshold value τ, construct the coarse-mesh using a given order, n, of interpolating functions in the approximate space V_j, solve the coarse-mesh problems, $K_0u_0 = f_0$. Compute relative error estimator ε_0.
2) Compare ε_0 with the threshold value τ, if $\varepsilon_0 \le \tau$, stop and give the answer.
3) For each interpolating function, construct new operator-orthogonal wavelets by the lifting scheme. Compute the operator-orthogonal wavelet solution and the relative error estimator ε_j according to Eq. (36).
4) If $\varepsilon_j \le \tau$, stop and give the answer.
5) Add lifted wavelets of the wavelet space W_{j+1} into initial multiresolution finite element space, and GOTO 3.

5. Numerical examples

As the common problems in structural mechanics, rod, bar and Timoshenko beam problems are computed by dynamic multiresolution algorithm using operator-orthogonal wavelets in the following numerical examples. The flexibility and accuracy of the operator-orthogonal wavelet solution are discussed in detail.

Example 1 Fig. 4 shows an axial rod subjected to distributed loading $q(x) = [200 - 40000(x-0.5)^2]e^{-100(x-0.5)^2}$, rod length $L = 1$ and physical parameter $EA = 1$.

It can be easily verified that the linear scaling functions are naturally orthogonal to the initial linear wavelets with respect to the operator of rod problem, so we select quadratic interpolation scaling functions to derive the lifted wavelets. Based on three basic principles, the appropriate coefficient vectors are chosen and new lifted wavelets can be constructed, correspondingly. Fig. 5 shows two lifted wavelets with only one vanishing moment and Fig. 6 shows two lifted wavelets with two vanishing moments. According to the necessary and sufficient condition for the complete wavelet space, we must choose two lifted wavelet bases on the support of one element. Given the threshold value $\tau = 0.05$, the problem is solved by the lifting scheme. Fig. 7 indicates the details of operator-orthogonal wavelet solution in each scale. Fig. 8 illustrates the sparsity pattern of the derived multiresolution stiffness matrix. The dotted lines separate the interaction and detail matrices at each scale. It can be seen that the multiresolution stiffness matrix is block-diagonal because of the decoupling of scaling function and lifted wavelets. Table 1 gives the error estimator and relative

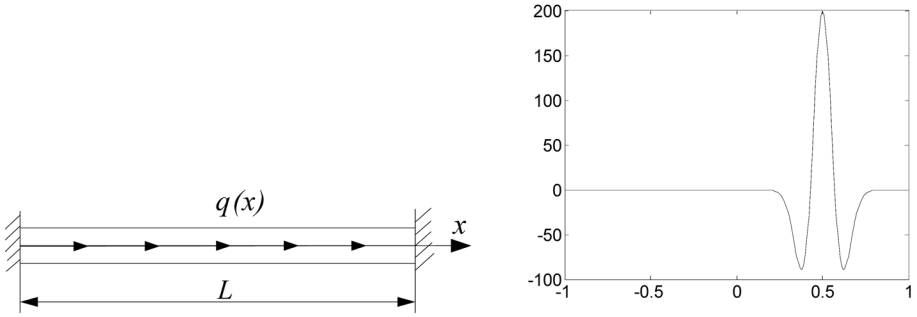

Fig. 4 An axial rod subjected to distributed loading $q(x) = [200 - 40000(x-0.5)^2]e^{-100(x-0.5)^2}$

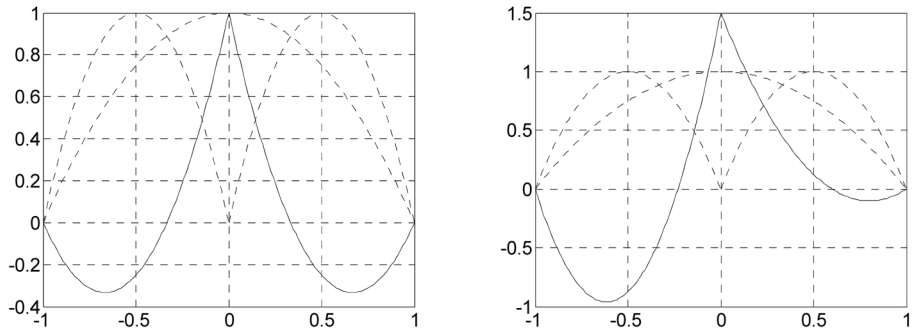

Fig. 5 Lifted wavelets for rod element with one vanishing moment

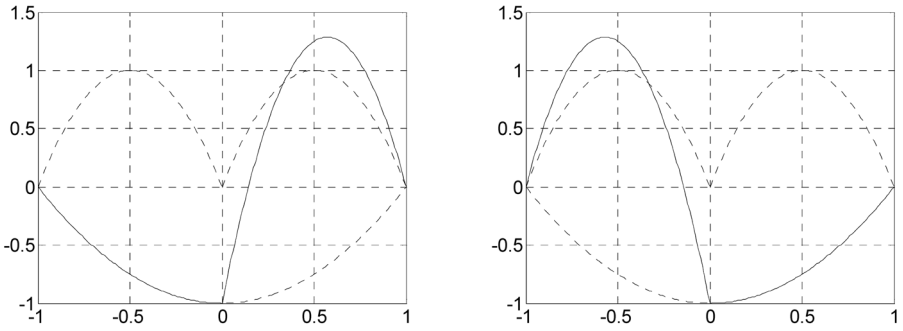

Fig. 6 Lifted wavelets for rod element with two vanishing moments

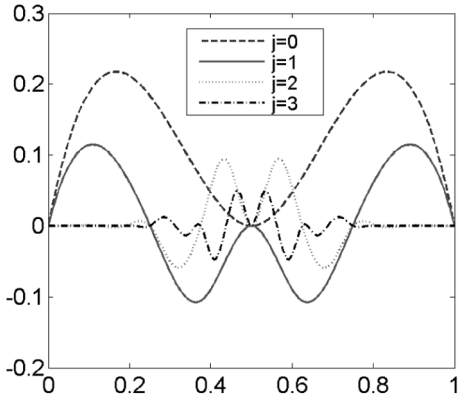

Fig. 7 The details of operator-orthogonal wavelet solution for axial bar

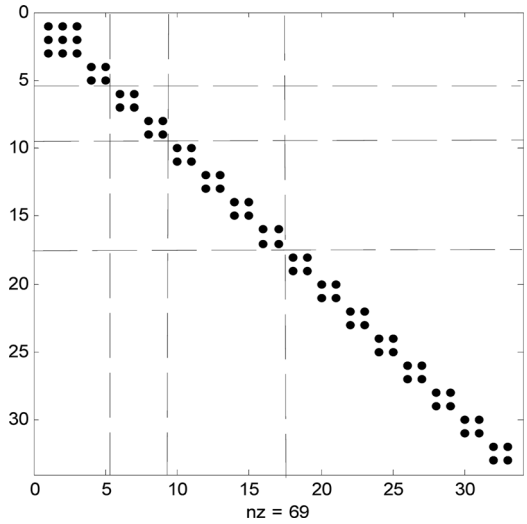

Fig. 8 Sparsity pattern of multiresolution stiffness matrix

Table 1 The operator-orthogonal wavelet solution of displacement for axial rod

Space	Error estimation	Relative error	DOFs
$V0(j = 0)$	-	-	3
$W0(j = 0)$	0.18353	0.69032	2
$W1(j = 1)$	0.11283	0.11283	4
$W2(j = 2)$	0.09354	0.09354	8
$W3(j = 3)$	0.04833	0.04834	16

error estimation in each scale for the operator-orthogonal wavelet solution. The number of scaling functions and lifted wavelets, also called degrees of freedom (DOFs), on each scale is also listed. It can be observed that the dynamic multiresolution algorithm using operator-orthogonal wavelets converges fast by adding new lifted wavelets.

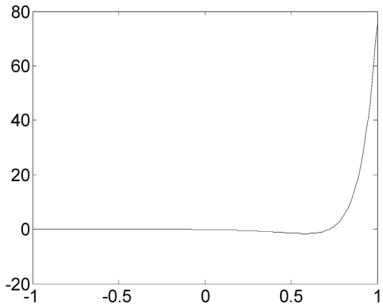

Fig. 9 The variable loading $q(x) = \frac{\theta^2}{(e^{\theta}-1)^2}(4e^{2\theta x} - e^{\theta x} - e^{\theta(x+1)})$ for torsional rod

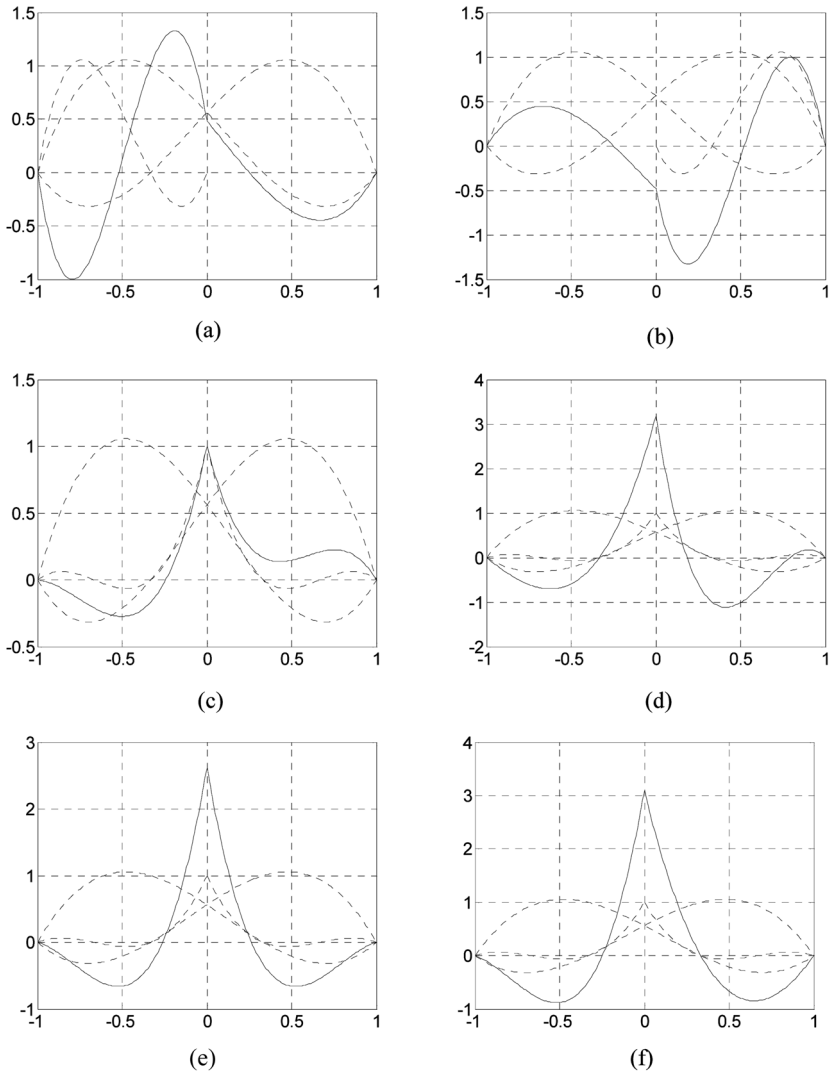

Fig. 10 Lifted wavelets operator-orthogonal with cubic interpolation functions

Example 2 A torsional bar is subjected to variable loading, which is fixed at both ends. Let bar length $L = 1$, physical parameter $GJ = 1$, the loading function $q(x)$ shown in Fig. 9 is selected corresponding to the solution $u(x) = \frac{1}{GJ}\frac{e^{\theta x}-1}{e^{\theta}-1}\left(1-\frac{e^{\theta x}-1}{e^{\theta}-1}\right)$, let $\theta = 5$.

In order to approximate the exact solution in fast convergence rate, we choose cubic interpolation scaling functions to derive the lifted wavelets. Based on three basic principles, the appropriate coefficient vectors are chosen and new lifted wavelets can be constructed, correspondingly. Figs. 10(a)-(c) shows three lifted wavelets with two vanishing moment and Figs. 10(d)-(f) shows three lifted wavelets with three vanishing moments. More lifted wavelets can also be constructed by assembling the scaling functions and wavelets. According to the necessary and sufficient condition for the complete wavelet space, we must choose three lifted wavelet bases on the support of one element.

Given the threshold value $\tau = 0.01$, the problem is solved by the lifting scheme. Fig. 11 shows the details of operator-orthogonal wavelet solution in each scale. Fig. 12 plots the multiresolution stiffness matrix and shows that multiresolution stiffness matrix is block-diagonal and highly sparse. Table 2 illustrates the error estimator and relative error estimation in each scale for the operator-orthogonal wavelet solution. It can be seen that the problem can be solved by adding new lifted wavelets with high convergent rate.

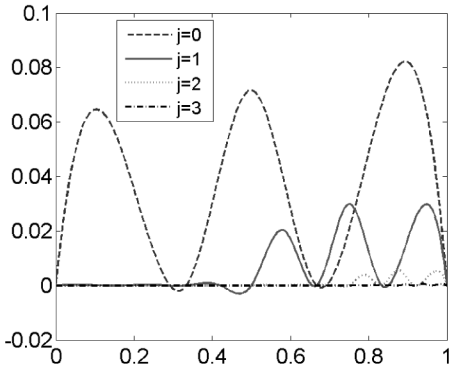

Fig. 11 The details of operator-orthogonal wavelet solution for torsional rod

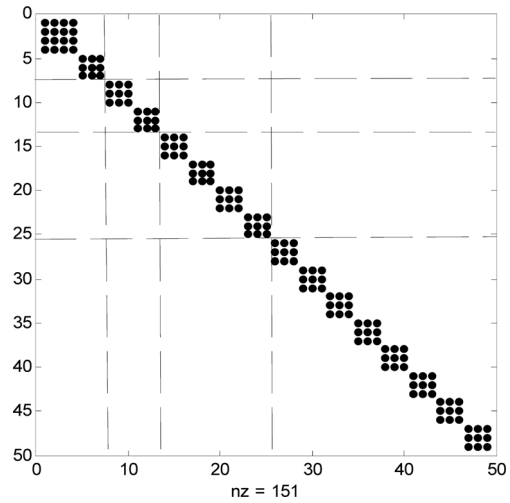

Fig. 12 Sparsity pattern of multiresolution stiffness matrix

Table 2 The operator-orthogonal wavelet solution of rotation for torsional rod

Space	Error estimation	Relative error	DOFs
$V0(j = 0)$	-	-	4
$W0(j = 0)$	0.07169	0.27004	3
$W1(j = 1)$	0.02358	0.13082	6
$W2(j = 2)$	0.00565	0.02271	12
$W3(j = 3)$	0.00064	0.00258	24

Example 3 Fig. 13 shows a rectangle cross-section cantilever beam subjected to distributed loading. The physical parameters and loading are: elastic modulus $E = 3.2 \times 10^{11}$ N/m^2, shear modulus $G = 8 \times 10^{10}$ N/m^2, width $B = 0.625$ m, height $H = 1$ m, shear correction coefficient $k_s = 5/6$, length $L = 10$ m, distributed loading $q(x) = q_0 \sin(\pi x/L)$ and $q_0 = 10^6$ N, respectively.

The multiresolution Timoshenko beam model is constructed to solve this problem. To avoid shear locking phenomenon in the solution of Timoshenko beam problem, we select consistent interpolation functions to derive the operator-orthogonal wavelets: transverse deflection and rotation are interpolated by quadratic and linear polynomials, respectively. In order to satisfy the four operators in the Timoshenko beam problem, we must solve a set of operators. For the scaling functions of transverse deflection, we can ensure the lifted wavelets in Fig. 5 and Fig. 6 can be operator-orthogonal to the scaling functions. For the scaling functions of rotation, we can not find the lifted wavelets that are operator-orthogonal to the scaling functions because two operators can not satisfied simultaneously. However, since the scaling functions are naturally operator-orthogonal to the wavelets, we can construct a sparse multiscale stiffness matrix.

Given the threshold value $\tau = 0.005$ for the transverse deflection, the problem is solved by the operator-orthogonal wavelets. Figs. 14(a)-(b) shows the transverse deflection and rotation details of operator-orthogonal wavelet solution in each scale. Fig. 15 illustrates the sparsity pattern of the multiresolution stiffness matrix and multiresolution stiffness matrix is highly sparse. Tables 3 and 4 illustrate the error estimator and relative error estimation in each scale for the operator-orthogonal

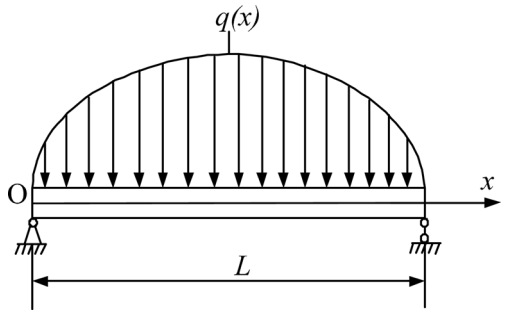

Fig. 13 A simply supported Timoshenko beam

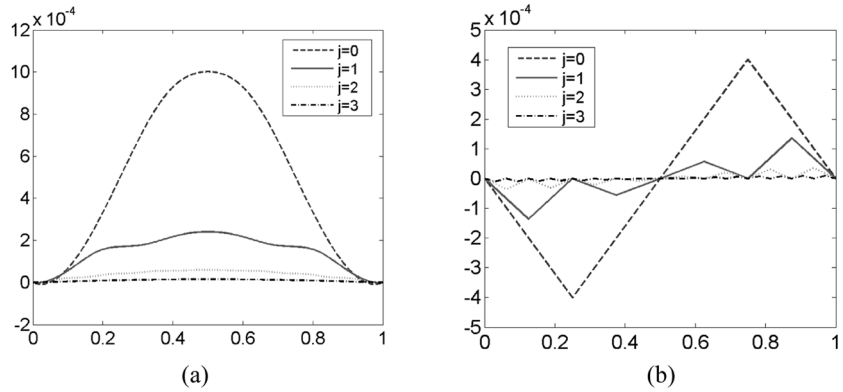

Fig. 14 The transverse deflection and rotation details of operator-orthogonal wavelet solution for Timoshenko beam

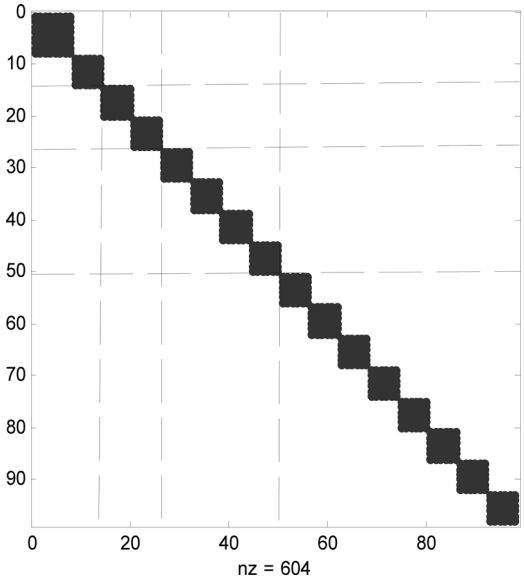

Fig. 15 Sparsity pattern of multiresolution stiffness matrix

Table 3 The operator-orthogonal wavelet solution of transverse deflection for Timoshenko beam

Space	Error estimation (10^{-3})	Relative error	DOFs
V0(j = 0)	-	-	5
W0(j = 0)	1.0019	0.16471	4
W1(j = 1)	0.2406	0.03805	8
W2(j = 2)	0.0596	0.00933	16
W3(j = 3)	0.0149	0.00232	32

Table 4 The operator-orthogonal wavelet solution of rotation for Timoshenko beam

Space	Error estimation (10^{-3})	Relative error	DOFs
V0(j = 0)	-	-	3
W0(j = 0)	5.8052	0.75000	2
W1(j = 1)	0.5444	0.07033	4
W2(j = 2)	0.1459	0.01885	8
W3(j = 3)	0.0371	0.00479	16

wavelet solution. The DOFs of transverse deflection and rotation on each scale are also given. It can be inferred that the exact solution of the Timoshenko beam problem can be approximated to any given threshold value by adding new lifted wavelets.

6. Conclusions

The operator-orthogonal wavelets are constructed based on the lifting scheme in the multiresolution finite element space and proved to be excellent decoupling bases in the structural

analysis. A dynamic multiresolution algorithm using lifted wavelets is developed to approximate the exact solution of structural problems in efficient manner. The lifting scheme provide an effective and flexible tool to custom design lifted wavelets to different kinds of structural problems. The further research is to develop Hermite and multi-dimensional lifting wavelets based on the lifting scheme to solve various engineering problems. It is promising that a great number of two- or three-dimensional lifting wavelets will solve general structural problems by using dynamic multiresolution algorithm accurately and efficiently. This work is currently under way.

Acknowledgements

The authors are very grateful to the anonymous referees for their important insight and comments, which helped greatly in improving the clarity and presentation of our original manuscript. The work in this article is supported by National Natural Science Foundation of China (No. 50875195), National High Technology Research and Development Program (No. 2009AA04Z406) and a Foundation for the Author of National Excellent Doctoral Dissertation of China (No. 2007B33).

References

Castrillón-Candàs, J. and Amaratunga, K. (2003), "Spatially adapted multiwavelets and sparse representation of integral equations on general geometries", *SIAM J. Sci. Comput*., **24**(5), 1530-1566.

Chen, C.M. and Huang, Y.Q. (1995), *High Accuracy Theory of Finite Element Methods,* Science and Technology Press, Hunan. (in Chinese)

Chen, X.F., Yang, S.J. and He, Z.J. (2004), "The construction of wavelet finite element and its application", *Finite Elem. Anal. Des.*, **40**, 541-554.

Davis, G.M., Strela, V. and Turcajova, R. (1999), *Multiwavelet Construction Via the Lifting Scheme, Wavelet Analysis and Multiresolution Methods*, Lecture Notes in Pure and Applied Mathematics (Ed. Marcel Dekker), New York.

D'Heedene, S., Amaratunga, K. and Castrillón-Candás, J. (2005) "Generalized hierarchical bases: a Wavelet-Ritz-Galerkin framework for Lagrangian FEM", *Eng. Comput.*, **22**(1), 15-37.

He, Y.M., Chen, X.F., Xiang, J.W. and He, Z.J. (2007), "Adaptive multiresolution finite element method based on second generation wavelets", *Finite Elem. Anal. Des.*, **43**, 566-579.

Ma, J.X., Xue, J.J., Yang, S.J. and He, Z.J. (2003), "A study of the construction and application of a Daubechies wavelet-based beam element", *Finite Elem. Anal. Des.*, **39**(10), 965-975.

Mallat, S.G. (1998), *A Wavelet Tour of Signal Processing*, Academic Press, Boston.

Pinho, P., Ferreira, P.J.S.G. and Pereira, J.R. (2004), "Multiresolution analysis using biorthogonal and interpolating wavelets", *IEEE Antenn. Propag. Soc. Symp*., **2**, 1483-1486.

Sudarshan, R., Amaratunga, K. and Grätsch, T. (2006), "A combined approach for goal-oriented error estimation and adaptivity using operator-customized finite element wavelets", *Int. J. Numer. Meth. Eng.*, **66**, 1002-1035.

Sweldens, W. (1997), "The lifting scheme: a construction of second generation wavelets", *SIAM J. Math. Anal.*, **29**(2), 511-546.

Vasilyev, O.V. and Bowman, C. (2000), "Second generation wavelet collocation method for the solution of partial differential equations", *J. Commun. Phys.*, **165**, 660-693.

Wang, X.C. (2002), *The Finite Element Methods*, Tsing Hua University Press, Beijing. (in Chinese)

Xiang, J.W., He, Z.J. and Chen, X.F. (2007), "Static and vibration analysis of thin plates by using finite element method of B-spline wavelet on the interval", *Struct. Eng. Mech.*, **25**(5), 613-629.